Tuijin Jishu/Journal of Propulsion Technology
ISSN: 1001-4055
Vol. 45 No. 4 (2024)

Insight into Adsorption Mechanism, Optimization and Modeling of Cationic Methylene Blue Dye Using a Chitosan/Analcime Clay Composite: Box-Behnken Design Application

Hibaterrahmane Yazi[1], Ammar Zobeidi[1,2], Douadi Ali[1], Eman Tidjani[3], Younes Moussaoui[4,5], Djamel Ghernaout[6,7], Noureddine Elboughdiri[6,8]

[1]*Pollution & Waste Treatment Laboratory (PWTL), University of Ouargla, PO Box 511, Ouargla 30000, Algeria.*

[2]*Laboratory of Applied Chemistry and Environment, Faculty of Exact Sciences, University of El Oued, 39000 El Oued, Algeria.*

[3]*Scientific and Technical Research Center in Physicochemical Analysis, University of Ouargla, Ouargla 30000, Algeria.*

[4]*Faculty of Sciences of Sfax, Organic Chemistry Laboratory (LR17ES08), University of Sfax, 3029 Sfax, Tunisia.*

[5]*Faculty of Sciences of Gafsa, University of Gafsa, 2112 Gafsa, Tunisia.*

[6]*Chemical Engineering Department, College of Engineering, University of Ha'il, PO Box 2440, Ha'il 81441, Saudi Arabia.*

[7]*Chemical Engineering Department, Faculty of Engineering, University of Blida, PO Box 270, Blida 09000, Algeria.*

[8]*Chemical Engineering Process Department, National School of Engineers Gabes, University of Gabes, Gabes 6029, Tunisia.*

Abstract

The facile synthesis of modificated chitosan/ Analcime clay (CTS/Ana) composite was performed by two subsequent steps involving modification of chitosan (CTS) with an inorganic clay (Analcime, Ana) from El Menia (El-Golea), Algeria. The applicability of the CTS/Ana composite for reduction of methylene blue dye (MB) from aquatic system was investigated. SEM and FTIR analyses were employed to identify the structural alterations in Ana clay matrix resulting from the incorporation of CTS and the adsorption of MB. The main key factors that influences the MB dye such as Ana loading 0–50% (A), CTS/Ana dose 0.02–0.1 g (B), solution pH 4–10 (C), temperature 30–60 °C (D), and contact time 5–45 min (E) were optimized by using Box–Behnken design (BBD). The highest MB dye removal (99.08 %) were observed at the following significant interactions: AB, AC, AD, BE, CE, and DE, under optimal conditions (A: 25%, B: 0.1 g, C: 10, D: 45 °C, and E: 25 min). The optimal adsorption capacity of 129.87 mg/g was attained for CTS/Ana composite at 45 °C under these settings. The Langmuir and pseudo-second-order models demonstrated efficacy for isotherms and kinetics, respectively. This work highlights that CTS/Ana composite offers great potential as a low-cost and effective biocomposite material for the organic dyes removal from water/ wastewater.

Keywords: Analcime clay, Chitosan, Box–Behnken design, Methylene blue dye.

1. Introduction

In contemporary society, effluent discharged by industries is a significant worry for environmentalists. Industrial effluents comprise numerous hazardous metals, deleterious gases, and a variety of organic and inorganic chemicals. The release of these untreated toxic effluents has compromised natural flora and wildlife and poses a threat to human health. Long-term exposure to such an environment can result in severe diseases, including cancer, delayed neurological responses, mutagenic alterations, and neurological problems [1]. Consequently, there is an ongoing requirement to uphold the standard permitted limits of these elements in industrial effluents prior to environmental disposal. Consequently, numerous physical, chemical, and biological approaches have been utilised to address the issue of removing these substances from wastewater [2-4]. Cationic dyes, especially methylene blue (MB), demonstrate greater toxicity compared to anionic dyes [5, 6]. Synthetic dyes, while offering stability, may be associated with health issues including allergic dermatitis, cancer, and genetic abnormalities [7, 8]. Various technologies, including biological and physico-chemical methods, membrane filtration, ozonation, advanced oxidation, and adsorption, are employed to treat wastewater containing dyes [9-17].

Adsorption is favoured over other costly procedures because of its adaptability, compatibility, affordability, and regenerative capacity [18, 19]. In light of contemporary trends in achieving environmental sustainability, scientists are focussing on employing naturally occurring materials to create cost-effective green adsorbents for the efficient elimination of harmful substances from wastewater [20, 21].

The use of several clay types as adsorbents has attracted attention due to their cost-effectiveness and local availability [22, 23]. The chemical and pore characteristics of clay minerals substantially affect their adsorption capabilities. Improvements in adsorption capacity have been achieved through chemical and physical modifications of pore structures. Inorganic bases, acids, surfactants, and salts have been employed to modify clay minerals, while a combination of chemical and physical treatments has been implemented to alter the surface and structure of these minerals [23, 24].

Recently, chitosan (CTS) , which is renewable, plentiful, and non-toxic, has been developed as a cost-effective and efficient alternative [25-27]. The positive charge and polysaccharide macromolecular structure of CTS render it effective for the elimination of anionic dyes [28, 29]. Acidic circumstances ($pH < 5$) render CTS unstable and rapidly dissolve it, hence restricting its application due to the protonation of amino groups. The molecular structure of CTS has been modified both physically and chemically to incorporate spherical beads, enhancing porosity and surface area [30].

This study evaluates the sorption efficacy of modified local clay, enhanced with additional surface functional groups via CTS coupling. Multivariate modeling and optimization of MB adsorption onto modified clay were performed using response surface approach, integrating critical parameters such as adsorbent dosage, solution pH, temperature, and contact duration, in addition to other input variables. Furthermore, thorough examinations were conducted on the adsorption kinetics, isotherms, and thermodynamics of MB dye removal employing the modified clay. A significant component of this work is the possibility for pollutant removal by the use of a novel bio-adsorbent, specifically a native clay from El Menia.

2. Materials and Methods

The clay sample (Ana) was collected from Hassi Gara, El Menia southeast Algeria. The dye used was the methylene bleu (MB) extended from Sigma-Aldrich. The commercial CTS was purchased by Sigma–Aldrich. Hydrogen peroxide (H_2O_2), Sodium acetate (CH_3COONa), Acetic acid (CH_3COOH), Sodium hexametaphosphate ($(NaPO_3)_6$), Hydrochloric acid (HCl), Sodium hydroxide (NaOH) were furnished from Merck. The Shimadzu UV-Visible Spectrophotometer UV-2600 was used to read the absorbances to determine the concentrations of dye. Sample characteristics were determined using scanning electron microscopy/energy-dispersive X-ray analysis (Hitachi, TM3030Plus, Tabletop Microscope), Fourier transform infrared analysis (Cary 600 series FT-IR spectrophotometer, Agilent technologies).

2.1. Dye solution The MB characteristics are illustrated in Table 1. The MB solution dye was prepared by dissolving 100 mg of dye in 1L of distilled water. Separated analyses were done at λ_{max} = 664 nm using a UV–Visible spectrophotometer.

Table 1. General characteristics of MB [31].

Name	Molecular formula	Mw (g mol^{-1})	Nature	λ_{max} (nm)
Methylene bleu	$C_{16}H_{18}ClN_3S$	373.90	Cationic	665

2.2. Preparation of samples

The clay sample fractionation method employed in this investigation is derived from previous research [32, 33]. The natural rock clay was subjected to a series of processes to acquire our samples. The clay was immersed in water and permitted to degrade entirely over 24 hours. It was then filtered using polypropylene cartridges with 5 µm apertures to isolate particles smaller than 5 µm. The resultant material was dried at 100 °C for 24 hours and then pulverized into a powder. Subsequently, to remove any organic compounds, the clay was washed with 40 cc of a 6% H_2O_2 solution. Subsequently, a solution containing 80 ml of buffer solution at pH 4.8, composed of 16 g of CH_3COONa and 10 ml of CH_3COOH, was introduced. Ultimately, to acquire particles smaller than 2 µm, a graduated tube was employed with the incorporation of $(NaPO_3)_6$. Following a settling duration of 7 hours and 45 minutes, a floating layer was obtained at a depth of 10 centimeters. The gathered samples were then rinsed several times with distilled water, centrifuged, and subsequently preserved for future utilization.

2.3. Synthesis of CTS/Ana

This study entailed the fabrication of a modified sample by amalgamating 1 g of CTS with 100 ml of 5% acetic acid. The liquid was incessantly stirred at ambient temperature until a gel was produced. Subsequently, 1 g of clay was added to the mixture, which was then continuously agitated for 24 hours. The mixture was incrementally added dropwise to a beaker containing 100 ml of a 0.5 M sodium hydroxide (NaOH) solution, resulting in the drops solidifying into pellets upon contact with the solution. The solution was subsequently filtered, and the pellets were thoroughly washed until the pH reached 7. The pellets were desiccated and meticulously stored until needed, with intentional segregation during the drying process to avoid adhesion [34, 35].

The ratio of clay to CTS must be considered during sample production. A 50% sample is prepared with a CTS /Ana ratio of 1:1, while a 25% sample is prepared using a ratio of 1/4:3/4.

2.4. Experimental design

The RSM Design-Expert is a distinct functionality within Stat-Ease's Design-Expert program. It emphasizes Response Surface Methodology (RSM) for the optimization of processes. It assists researchers in designing experiments, fitting response surface models, and analyzing data effectively [36, 37]. This study conducted forty-one tests to evaluate the influence of five primary parameters (acid activation concentration, adsorbent injection, pH, residence time, and temperature) on methylene blue elimination. Optimal parameters were established by exploratory research, and the experimental domain was delineated using Box-Behnken design (BBD). The Stat-Ease Design-Expert software (Version 13.0) was utilized for MB reduction. Table 2 displays the magnitudes and coded values of independent variables. Initial assessments established their scope. The experimental findings were analyzed, and the clearance of MB dye was anticipated using equation (1).

$$\Upsilon = \beta_0 + \sum_{i=1}^{k} \beta_i \, \mathcal{X}_i + \sum_{i=1}^{k} \beta_{ii} \, \mathcal{X}_i^2 + \sum_{i=1}^{k} \sum_{j=1}^{k} \beta_{ij} \, \mathcal{X}_i \mathcal{X}_j + \mathcal{E} \quad (1)$$

Where, ϒ represents the objective, *k* is the number of variables, *i* and *j* are the variable indices, β_0 is the constant coefficient, β_i and β_{ii} are linear and quadratic coefficients, β_{ij} is the interaction coefficient, and $\mathcal{E}$ is a random error. X_i and X_j are the response and coded values for independent factors (-1, 0, and +1), respectively. Positive coefficients show synergy, while negative ones indicate antagonism between variables.

Table 2. Coded and actual variables and their levels in BBD

Factor	Level		
	Low	Medium	High
CTS loading (%)	0	25	50
Adsorbent dose (g)	0.02	0.06	0.1
pH	4	7	10
Temperature (°C)	30	45	60
Contact time (min)	5	25	45

Researchers employed Analysis of Variance (ANOVA) to evaluate the model's accuracy by examining the coefficients, which included p-value, F-value, determination coefficient (R^2), projected determination coefficient (R^2_{pred}), adjusted determination coefficient (R^2_{adj}), acceptable precision, degrees of freedom (df), and standard deviation (SD) [38]. These characteristics were essential in assessing the accuracy of both the experimental data and the model. The researchers utilized a dependable second-order quadratic model equation to forecast optimal values and examine the interrelationships among the variables. Optimal factor values were established utilizing the regression equation, counter-response surface map, and limitations on variable levels. Initial tests were performed to ascertain extreme variable values.

2.5. Batch adsorption studies

The RSM Design-Expert was utilized to assess the adsorption capability of clay for the removal of MB dye. Various dye concentrations (50 to 300 mg/L) and adsorbent quantities (0.02 to 0.1 g), modified by CTS (25, 50%), were employed at diverse temperatures (30-60 °C) and pH levels (4-10), adjusted using 0.1M HCl and NaOH, during varying durations (5-45 min). Following the adsorption experiments, residual concentrations were quantified at λ_{max} 664 nm utilizing a UV-vis spectrophotometer. The adsorption capacity (q_e mg/g) and dye removal percentage (R%) were calculated using equations (2) and (3), respectively, after centrifuging the samples prior to measurement.

$$R(\%) = \frac{C_0 - C_e}{C_0} \times 100 \quad (2)$$

$$q_e = \frac{V}{W}\,(C_0 - C_e) \quad (3)$$

In order to C_0 (mg/L) are the initial MB dye concentrations and C_e (mg/L) are the equilibrium one, V (L) is the volume of the dye solution, and W(g) is the clay weight.

3. Results and Discussion

3.1. Characterization of CTS/Ana

The Fig. 1**.** below presented the SEM/EDX spectrum of modified local clay (a) befor, (b) after the adsorption of the MB dye. The Ana clay changed The SEM shows a coarse, porous surface with random fissures. Its massive dye-molecule interaction surface. Larger surface areas enhance dye-adsorbent interaction and adsorption. C, O, Mg, Al, Si, K, Fe, and Sr in EDX spectra resemble CTS-modified Ana clay. CTS and clay affect peak intensity. The EDX spectrum displays a bromine signal after MB dye removal, confirming dye adsorption. Bromine in modified clay confirms MB dye. Before and after dye removal, EDX spectra show minor element strengths and variations. Differences reflect adsorption-influenced elemental distribution. Dye molecules can displace ions or establish bonds. Use 25% CTS-modified Ana clay to remove SEM and EDX dye. Bromine absorbs contaminants through its porous surface and essential components following dye removal. MB and CTS/Ana clay may increase elemental composition adsorption.

Table 3. The RSM Design-Expert matrix with five factors and experimental results for MB

Run	CTS loading (%)	Absorbent dose (g)	pH	Temperature (°C)	Time (min)	Removal (%)
12	25	0,06	4	30	25	43,61
23	25	0,02	7	30	25	69.34
30	25	0,1	7	30	25	78.55
31	25	0,06	7	30	5	44.47
32	25	0,06	10	30	25	87.64
36	50	0,06	7	30	25	47.76
44	0	0,06	7	30	25	92.01
46	25	0,06	7	30	45	80.86
1	0	0,06	7	45	5	34.72
2	25	0,1	7	45	45	98,18
3	25	0,06	7	45	25	97.43
4	50	0,06	4	45	25	34.02
6	25	0,1	7	45	5	48.83
7	25	0,02	7	45	45	71.33
8	25	0,06	10	45	5	48.04
9	50	0,06	10	45	25	57.66
10	25	0,02	4	45	25	44.87
13	25	0,1	4	45	25	48.92
14	25	0,02	10	45	25	75.20
17	25	0,06	7	45	25	97.43
18	25	0,06	4	45	45	46.31
19	25	0,06	10	45	45	98.28
20	25	0,02	7	45	5	33.74
21	50	0,02	7	45	25	45.13
22	0	0,1	7	45	25	94.80
24	25	0,06	7	45	25	97.43
26	0	0,06	7	45	45	90.62
27	50	0,06	7	45	45	48.15
28	0	0,02	7	45	25	63.09
29	50	0,06	7	45	5	34.42
34	25	0,06	7	45	25	97.43
35	25	0,06	4	45	5	28.78
37	25	0,1	10	45	25	99.08
38	0	0,06	4	45	25	51.30

39	25	0,06	7	45	25	97.43
41	0	0,06	10	45	25	81.75
42	25	0,06	7	45	25	97.43
45	50	0,1	7	45	25	51.01
5	25	0,02	7	60	25	52.98
11	25	0,06	10	60	25	65.01
15	25	0,06	4	60	25	40.12
16	25	0,1	7	60	25	67.92
25	0	0,06	7	60	25	60.42
33	25	0,06	7	60	5	30.62
40	25	0,06	7	60	45	70,85
43	50	0,06	7	60	25	41.89

The FTIR spectra in Fig. 2 illustrate the CTS/Ana-25 prior to (a) and subsequent to (b) methylene blue (MB) dye removal, indicating alterations in dye adsorption. A prominent band around 3400 cm^{-1} likely corresponds to hydroxyl stretching vibrations from CTS and adsorbed water, whereas a band about 1650 cm^{-1} may indicate amide I and water bending vibrations prior to dye removal. The 1000-1100 cm^{-1} range signifies T-O stretching vibrations inside the clay framework, whereas the 500-600 cm^{-1} bands are associated with structural vibrations or interactions with CTS [39-41]. The removal of dye leads to a diminished intensity of the OH band at 3400 cm^{-1}, signifying interactions with hydroxyl groups or adsorbed water, alongside a reduction in water content or modified amide group interactions at 1650 cm^{-1}. Subtle fluctuations in the 1000-1100 cm^{-1} range signify structural modifications in the clay framework due to dye adsorption, whereas alterations in the 500-600 cm^{-1} region reflect the reorganization of CTS complexes [33]. Spectra indicate that methylene blue adsorption influences hydroxyl and amide groups, reduces water content, and partially alters the Ana structure.

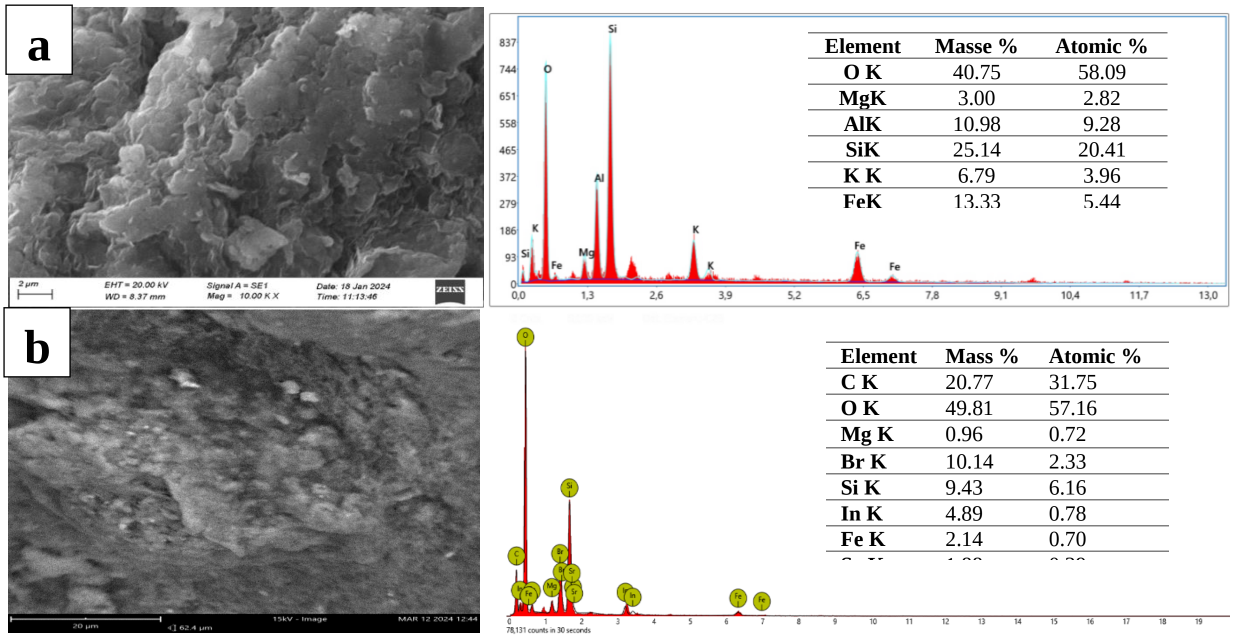

Fig. 1. SEM and EDX spectrum of CTS/Ana-25 (a) before and (b) after MB dye removal.

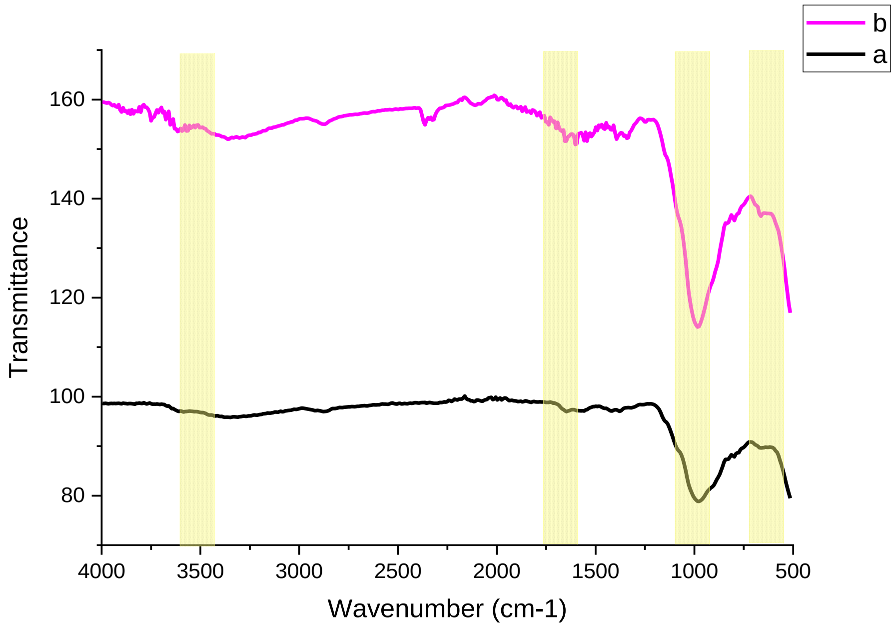

Fig. 2. FTIR spectra of CTS/Ana-25 (a) before and (b) after MB dye removal

3.2. Parametric optimisation with BBD-RSM

Utilizing a BBD, we evaluated the singular and synergistic effects of A: CTS loading, B: adsorbent dose, C: solution pH, D: temperature, and E: contact time on the removal of MB dye. The experimental results' statistical significance was validated by analysis of variance (ANOVA), which indicated an F-value of 71.62 and a highly significant p-value of <0.0001 (Table 5). The results, as emphasized by reference [42], demonstrate the significant statistical relevance of the BBD model in the context of MB dye elimination. A coefficient of determination $R^2 = 0.98$ indicates a strong correlation between the observed and predicted amounts of MB dye elimination. The importance of the BBD model's components is clear, as variables A, B, C, D, E, AB, AC, AD, BE, CE, DE, A^2, B^2, C^2, D^2, and E^2 exhibited statistical significance (p-value < 0.05) under the designated experimental conditions. These data validate the significance of these parameters in the context of MB elimination. Excluding terms with p-values exceeding 0.05, the quadratic polynomial equation (4) effectively delineates the link among the examined parameters (CTS loading, dose, pH, temperature, contact time) and MB dye elimination in the BBD model. This guarantees a more precise alignment of the model with the experimental data.

$$MB\ removel(\%) = +97.43 - 13.86A + 8.23B + 17.93C - 7.15D + 17.15E - 6.46AB - 7.16AC + 6.43AD + 4.96BE + 8.18CE - 4.78DE - 20.46A^2 - 12.15B^2 - 22.20C^2 - 17.89D^2 - 19.82E^2 \quad (4)$$

Table 5. Analysis of variance (ANOVA) of the MB dye removal response surface quadratic model

Source	Sum of Squares	df	Mean Square	F-value	p-value
Model	23741.24	20	1187.06	71.62	< 0.0001
A-CTS loading (%)	3074.70	1	3074.70	185.51	< 0.0001
B-Absorbent dose (g)	1082.57	1	1082.57	65.32	< 0.0001
C-Time	5141.97	1	5141.97	310.24	< 0.0001

D-Temperature	818.39	1	818.39	49.38	< 0.0001
E-pH	4703.56	1	4703.56	283.79	< 0.0001
AB	166.80	1	166.80	10.06	0.0040
AC	205.06	1	205.06	12.37	0.0017
AD	165.38	1	165.38	9.98	0.0041
AE	13.00	1	13.00	0.7841	0.3843
BC	34.57	1	34.57	2.09	0.1611
BD	8.21	1	8.21	0.4952	0.4881
BE	98.31	1	98.31	5.93	0.0223
CD	3.69	1	3.69	0.2224	0.6413
CE	267.49	1	267.49	16.14	0.0005
DE	91.58	1	91.58	5.53	0.0269
A^2	3652.82	1	3652.82	220.39	< 0.0001
B^2	1288.56	1	1288.56	77.75	< 0.0001
C^2	4302.84	1	4302.84	259.61	< 0.0001
D^2	2794.55	1	2794.55	168.61	< 0.0001
E^2	3426.99	1	3426.99	206.77	< 0.0001
Residual	414.35	25	16.57		
Lack of Fit	414.35	20	20.72		
Pure Error	0.0000	5	0.0000		
Cor Total	24155.59	45			

Normal probability plots of externally assessed residuals examine the normality of the residual distribution in Fig 3a. Statistics assumes normal residuals for precise predictions. Due to the alignment of points, both representations exhibit normal residuals. This pattern upholds model assumptions such as residual independence and the plausibility of hypotheses. Normal residuals indicate correlations that enhance model prediction. The randomness and independence of residuals with relation to the run number are depicted in Fig. 3b. Model autocorrelation and bias are absent, as all residuals reside within the residual rings and exhibit no discernible patterns or trends over run numbers. Post-randomization, the stable model accurately forecasts MB dye removal parameters devoid of overfitting or systemic errors. This assesses the model's efficacy in dye removal. Ultimately, Fig 3c juxtaposes the actual and anticipated removal of MB dye. Robustly interconnected data forecasting models perform effectively. The proximity of the actual and anticipated values indicates a minimal model-experimental error. A robust correlation enhances the model's ability to predict and optimize MB dye removal [42, 43].

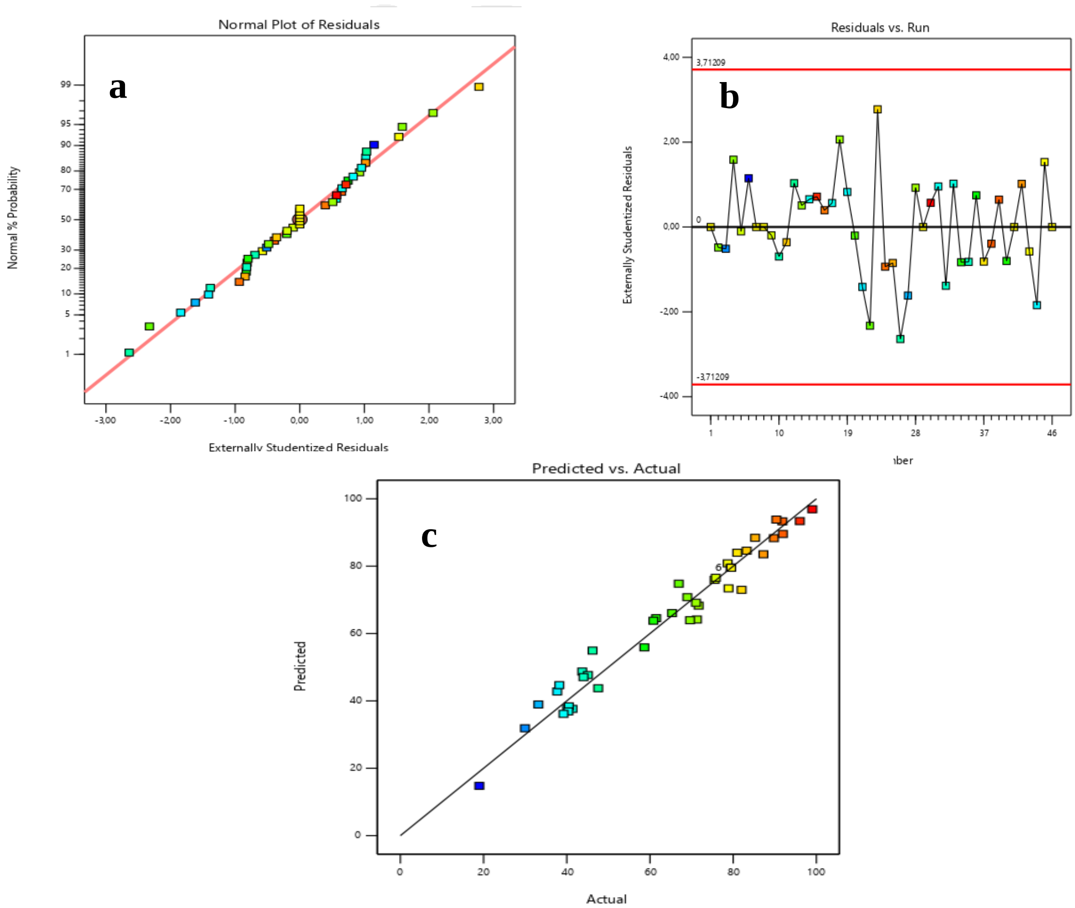

Fig. 3. Plots of (a) the normal (%) probability of residuals, (b) residuals vs. the run order, and (c) actual values vs. predicted values

Fig. 4. presents two 3D surface plots, depicting the relationship between various factors and the efficiency of MB elimination. Plot (a) in Fig. 4 illustrates that dye removal increases with absorbent dosage ranging from 0.02 to 0.1 g and CTS loading from 0 to 25%. Both criteria are essential for process optimization. In figure (b), the efficacy of removal enhances over time (5–45 minutes) and with CTS loading; nevertheless, the effect levels out, indicating an optimal range for both variables. Dye clearance escalates with CTS (0–50%) and temperatures of 30–60°C in plot c. The influence of temperature diminishes as values increase, suggesting an optimal range. In plot (d), elevating the pH from 4 to 10 and incorporating 0.02 to 0.1 g of absorbent eradicates color and enhances adsorption. The efficiency of dye removal increases with pH, but time levels out beyond a certain threshold (Plot e). Ultimately, plot (f) illustrates that pH effectively removes dye more efficiently at lower temperatures. The removal of dye is primarily influenced by pH, CTS loading, and absorbent dosage. CTS-modified Ana effectively eliminates MB.

3.3. Adsorption Study We investigated the effect of contact duration on the adsorption of MB dye onto activated carbon (AC), examining various starting concentrations ranging from 50 to 300 mg/L. The research upheld consistent parameters for CTS loading (25%), adsorbent dosage (0.1 g/100 mL), solution pH (10), and temperature (45 °C). Fig. 5 illustrates graphs of changed clay adsorption capacity (mg/g) with time (min) for different initial concentrations of MB dye. The adsorption capacity escalated from 25.61 to 138.24 mg/g when the MB dye concentration grew from 50 to 300 mg/L. This trend indicates a substantial driving force, ascribed to a concentration gradient, affecting the movement of MB dye molecules into the internal pores and active sites of the modified clay [44].

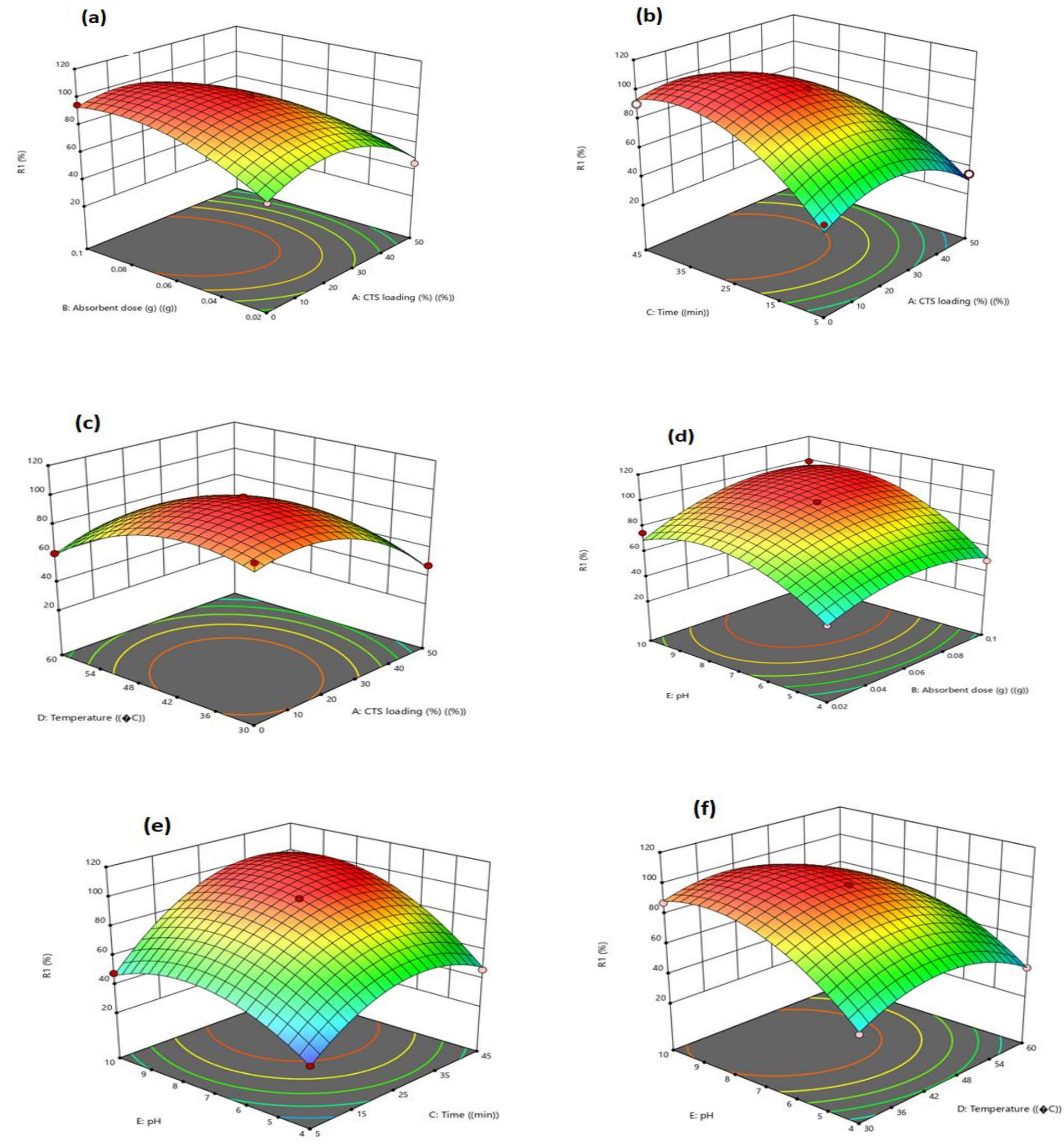

3.4.

Fig. 4. The 3D surface plot displays (a) interaction between the dose and CTS loading, (b) shows interaction between the contact time and the CTS loading, (c) showing interaction between temperature and CTS loading, (d) interaction between pH and the absorbent dose, (e) interaction between pH and contact

time, and (f)showing interaction between the pH and the temperature.

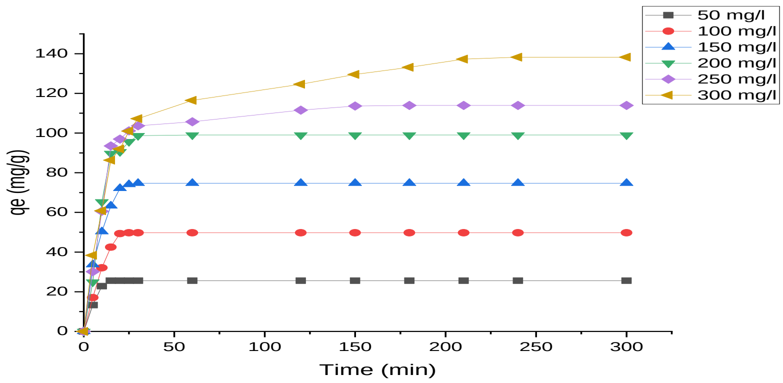

Figure 5. Effect of the initial MB concentration on the modified clay adsorption capacity as a function of the contact time (pH =10, adsorbent dose = 0.1 g, agitation speed = 100 rpm and volume of solution = 100 mL).

3.5. Adsorption kinetics

The adsorption kinetics are essential for understanding the adsorption behavior of Methylene Blue (MB) on the modified clay surface and for examining the underlying adsorption process. To this end, both the pseudo-first-order (PFO) and pseudo-second-order (PSO) kinetic models were utilized [45]. The non-linear representations of the kinetic models, delineated in equations 6 and 7, are as follows:

$$q_t = q_e(1 - e^{-k_1 t}) \quad (6)$$

$$q_t = \frac{q_e^2 k_2 t}{1 + q_e k_2 t} \quad (7)$$

where:

q_t (mg/g) is the amount of MB dye adsorbed at time t (min), k_1 (1/min) is the rate constant of PFO, k_2 (g/mg.min) is the rate constant of PSO.

Table 6. The kinetic parameters of pseudo-first-order (PFO) and pseudo-second-order (PSO) for MB sorption onto AC at optimal conditions

Concentration (mg/l)	q_e exp (mg/g)	Pseudo-First-Order			Pseudo-Second-Order		
		q_e cal (mg/g)	K1 (1/min)	R^2	q_e cal (mg/g)	K_2 (g/mg*min)	R^2
50	25.61	58.45	0.3111	1	31.06	0.0019	1
100	49.75	167.07	0.2676	0.87	50.25	0.0003	0.99
150	74.72	168.16	0.2101	0.96	80.00	0.0009	0.99
200	99.03	414.1	0.2156	0.91	105.26	0.0008	0.99
250	113.94	29.33	0.0264	0.93	116.28	0.0021	1
300	138.24	73.49	0.0175	0.93	140.85	0.0006	0.99

The data in Table 6 indicates that the pseudo second order model more accurately describes the adsorption of MB dye on the modified clay surface than the pseudo first order model. The finding is substantiated by the elevated correlation coefficients (R^2) derived from the PSO model, signifying a more robust concordance between the model predictions and experimental data. The computed "q_e cal" values from the PSO model closely align with the experimental "q_e exp" values, indicating enhanced prediction accuracy relative to the PFO model. This indicates that the adsorption of MB dye on the modified clay surface is predominantly controlled by the chemisorption process, as outlined by the PSO model.

3.6. Adsorption isotherm

Adsorption isotherms like as Langmuir, Freundlich, and Temkin are crucial for comprehending the interaction of MB dye molecules with activated carbon. These models facilitate the analysis of equilibrium adsorption data and effectively ascertain activated carbon adsorption capacity[46-48]. The non-linear representations of the isotherms are delineated in Eqs. (8), (9), and (10) as follows:

Langmuir	Freundlich	Temkin
$\frac{C_e}{q_e} = \frac{q_{max}K_aC_e}{1+K_aC_e}$ (8)	$q_e = K_f C_e^{\frac{1}{n}}$ (9)	$q_e = \frac{RT}{b_t}(lnK_tC_e)$ (10)

where: Ce (mg.L^{-1}) is the concentration of MB dye at equilibrium, q_{max} (mg.g^{-1}) is the maximum quantity of the MB dye per unit mass of CTS/Ana, q_e (mg.g^{-1}) is the amount of MB dye uptake at per unit weight of CTS/Ana, K_a (L.mg^{-1}) is Langmuir constant, K_F (mg.g^{-1})(L.mg^{-1})$^{1/n}$ is the Freundlich constant, n is the dimensionless constant that indicates the adsorption intensity, K_T (L/mg) is Temkin constant, T (K) is temperature, R (8.314 J/mol.K) is the universal gas constant, and b_T (J/mol) represent adsorption intensity and heat of adsorption.

Table 7. Langmuir, Freundlich, and Temkin constants for the adsorption of MB dye onto CTS/Ana at 45 °C

Model	Parameters	Value
Langmuir	q_{max} (mg.g^{-1})	129.87
	K_a (L.mg^{-1})	1.79
	R^2	0.99
Freundlich	K_F (mg.g^{-1})(L.mg^{-1})$^{1/n}$	65.05
	n	4.10
	R^2	0.75
Temkin	K_T (L/mg)	71.98
	b_T (J/mol)	34.97
	R^2	0.89

The adsorption of MB dye by the modified clay, as shown in Table 7, is most effectively conveyed by the Langmuir adsorption isotherm model, which demonstrates a superior R^2 value (0.99) relative to the Freundlich and Temkin models. This indicates that MB dye molecules establish a monolayer covering on the uniform surface of the adsorbent, featuring energetically comparable sites[49]. Additionally, the Langmuir model indicated that the maximum adsorption capacity (q_{max}) for the modified clay is 129.87 mg/g. This value denotes the maximum quantity of MB dye that may be absorbed per unit mass of modified clay under ideal conditions.

Modified clay has proven to be a highly efficient adsorbent for the elimination of the cationic dye (MB) from water, as evidenced by a comparison of its q_{max} with other adsorbents documented in the literature presented in Table 8.

Table 8. Adsorption capacities of different adsorbents

Adsorbents	q_{max}(mg/g)	References
Chitosan-ECH/kaolin composite	560.90	[50]
CC25	254.8	[33]
Fe_3O_4-CTMAC/SEIA-Mt	246	[51]
IKaol Algerian	114.94	[43]
Activated carbon/cellulose composite (ACC)	103.66	[52]
CTS-AC	56.7	[53]
Coconut husk cellulose	42.72	[42]
Gypsum	36	[7]
CTS/Ana	129.87	This study

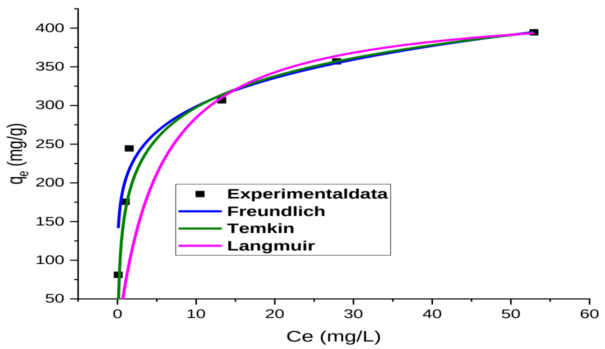

Fig. 6. Adsorption isotherm models of the MB dye onto CTS/Ana-25 (pH =10, adsorbent dose = 0.1 g, agitation speed = 100 rpm and volume of solution = 100 mL).

3.7. Adsorption thermodynamics

Thermodynamic metrics such as ΔG°, ΔS°, and ΔH° are employed to evaluate the adsorption of MB dye onto the surface of activated carbon. ΔG° denotes spontaneity (negative values suggest feasibility), ΔS° quantifies unpredictability (positive values reflect increased disorder), and ΔH° represents thermal changes (negative for exothermic processes, positive for endothermic processes). These characteristics provide insights into the energetics and dynamics of the adsorption process, facilitating its optimization and comprehension. Thermodynamic characteristics of adsorption were derived using formulae. (11) to (13) [54]:

$$\Delta G^{\circ} = -RTLnK_d \quad (11)$$

$$K_d = \frac{q_e}{C_e} \quad (12)$$

$$LnK_d = \frac{\Delta S^{\circ}}{R} - \frac{\Delta H^{\circ}}{RT} \quad (13)$$

Thermodynamic parameters (ΔH˚ and ΔS˚) obtained from the lnKd against 1/T in Fig. 7, where the slope indicates ΔH˚ and the intercept signifies ΔS˚.

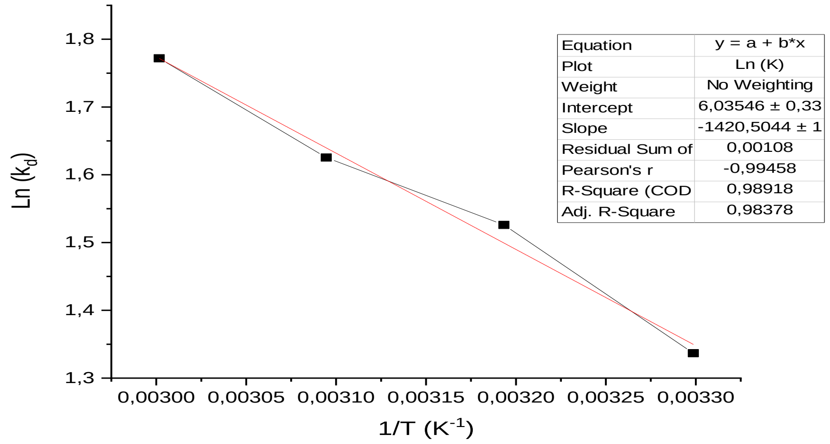

Fig. 7. Van't Hoff plot elucidates MB adsorption onto modified local clay thermodynamics.

The negative ΔG°, ΔH, and positive ΔS values associated with the methylene blue removal reaction using CTS/Ana, as detailed in Table 9, signify a spontaneous, exothermic, and entropy-increasing process. The negative ΔG° implies the reaction occurs autonomously, while the negative ΔH denotes heat release during the process [55]. The positive ΔS reflects an increase in disorder, likely resulting from new bond formation or a rise in particle quantity [55]. Collectively, these thermodynamic parameters indicate that methylene blue removal is a favorable process for effective pollutant elimination [56].

Table 9. Thermodynamic analysis of MB dye adsorption onto CTS/Ana.

T(K)	Ln (Kd)	ΔG° (KJ/mol)	ΔH° (KJ/mol)	ΔS° (KJ/mol)
303,15	1,337	-3,37	11,81	0,0502
131,15	1,526	-3,97		
323,15	1,626	-4,37		
333,15	1,772	-4,91		

3.8. Adsorption mechanism of MB

The Fig. 8 presented the adsorption mechanism of MB by CTS/Ana-25. The proposed process for the adsorption of MB by the modified clay involves a complex interaction between the functional groups on the adsorbent's surface and the dye molecules. Adsorption is predominantly influenced by the electrostatic interactions between the positively charged MB dye molecules and the negatively charged regions on the modified clay surface. Moreover, adsorption can be augmented by π-π interactions, wherein the electrons of the oxygen atom delocalize into the π orbital of the MB aromatic ring [57]. The existence of dipole-dipole hydrogen bonding between oxygen atoms on the modified clay and oxygen/nitrogen atoms in the molecular structure of MB, along with Yoshida hydrogen bonding between surface hydroxyl (-OH) groups and the MB aromatic ring, significantly influences the adsorption process [33, 58]. These interactions underscore the critical role of surface functional groups in augmenting the adsorption of MB dye on the modified clay. This offers essential insights for formulating adsorption techniques across various domains, including wastewater treatment and the elimination of dyes from industrial effluents.

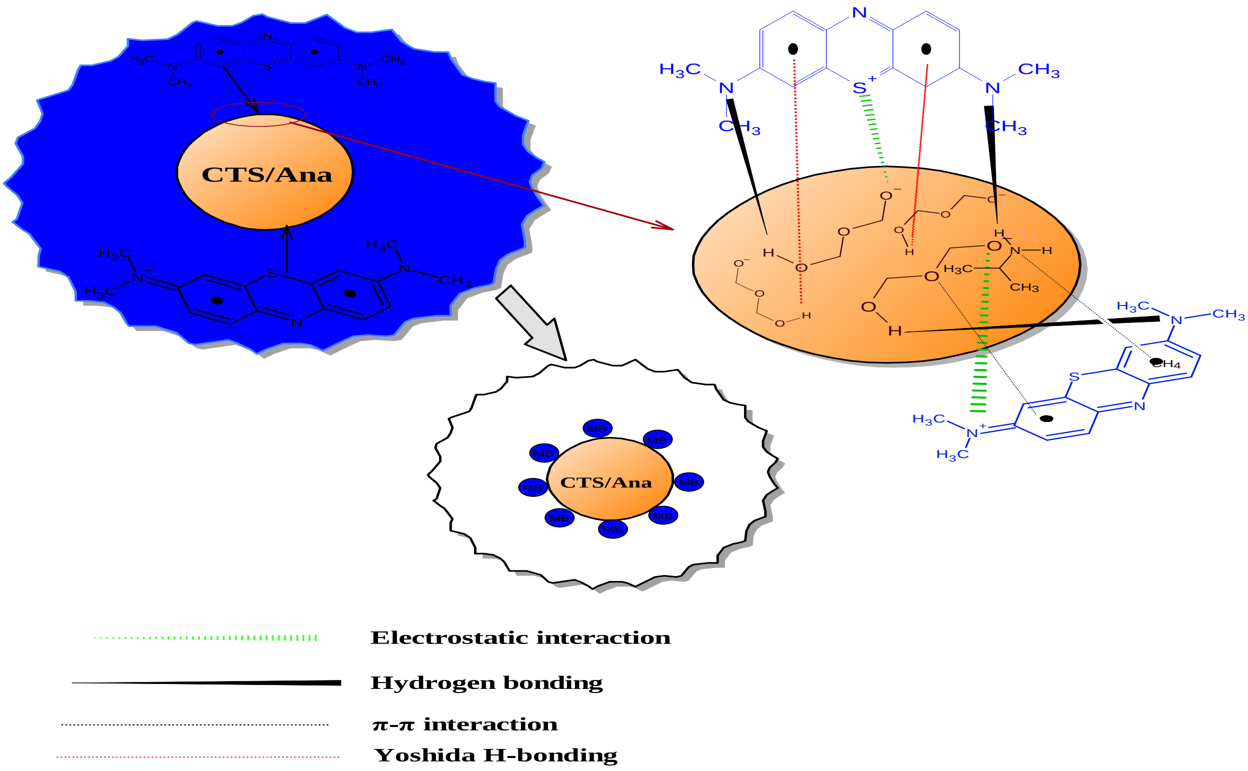

Fig. 8. Mechanism diagram of MB on the CTS/Ana surface.

4. Conclusion

This study assessed the efficacy of natural and modified local clay, in conjunction with 25% CTS, for the extraction of MB from water, utilizing Response Surface Methodology (RSM) to adjust the process parameters. The research aimed to determine the ideal conditions for improving MB removal utilizing clay-based adsorbents. The Box-Behnken design methodology was employed to determine the optimal adsorption parameters, analyzing the impacts of five independent variables. The study revealed that under the defined optimal conditions (CTS loading 25%, adsorbent dosage 0.1 g, pH 10, temperature 45 °C, and contact time 25 min), the highest removal rate of MB attained was 99.08%, accompanied by an optimal adsorption capacity of 129.87 mg/g. The adsorption process followed pseudo-second-order kinetics, as evidenced by the analysis of kinetic experimental data. The thermodynamic functions demonstrate that the adsorption process is both endothermic and spontaneous. The adsorption experiments demonstrated that the modified clay is an effective and cost-efficient adsorbent for the elimination of cationic dyes from diverse wastewater sources. These findings underscore the efficacy and cost-effectiveness of CTS/Ana-25 as a method for alleviating dye pollution in various industrial effluents and wastewater treatment systems.

Acknowledgments

The authors would like to thank the Algerian Ministry of Higher Education and Scientific Research and General Directorate of Scientific Research and Technological Development (DGRSDT) for their support and the necessary facilities to carry out this research.

Credit author statement

Hibaterrahmane Yazi: Ideation, Methodology, Research, Analysis of Data, Visualization, Preparing, Reviewing and Editing Original Draft. **Ammar Zobeidi**: Supervision, Ideation, Methodology, Software, Research, Analysis of Data, Visualization, Preparing, Reviewing and Editing Original Draft. **Douadi Ali**: Supervision assistant, Conceptualization, Investigation, Data curation. **Eman Tidjani:** Methodology, Reviewing and Editing. **Younes Moussaoui** and **Djamel Ghernaout:** Writing review & editing. **Noureddine Elboughdiri:** Conceptualization, Writing & editing. All authors have read and agreed to the published version of the manuscript

Data availability: All data and materials are viable.

Declarations

Ethics approval and consent to participate: All authors approved.

Consent for publication: All authors agree to the publication.

Competing interests: The authors declare no competing interests.

References

[1] V. Balaji, S. Datta, and C. Bhattacharjee, "Evaluation on biological treatment for industrial wastewater," *Biomed. Environ. Sci*, vol. 85, pp. 320-326, 2005.

[2] A. García-García, V. Martínez-Miranda, I. G. Martínez-Cienfuegos, P. T. Almazán-Sánchez, M. Castañeda-Juárez, and I. Linares-Hernández, "Industrial wastewater treatment by electrocoagulation–electrooxidation processes powered by solar cells," *Fuel*, vol. 149, pp. 46-54, 2015.

[3] M. M. Islam, M. N. Khan, S. Biswas, T. R. Choudhury, P. Haque, T. U. Rashid, *et al.*, "Preparation and characterization of bijoypur clay-crystalline cellulose composite for application as an adsorbent," *Adv. Mater. Sci*, vol. 2, pp. 1-7, 2017.

[4] D. B. Miklos, C. Remy, M. Jekel, K. G. Linden, J. E. Drewes, and U. Hübner, "Evaluation of advanced oxidation processes for water and wastewater treatment–A critical review," *Water research*, vol. 139, pp. 118-131, 2018.

[5] O. J. Hao, H. Kim, and P.-C. Chiang, "Decolorization of wastewater," *Critical reviews in environmental science and technology*, vol. 30, pp. 449-505, 2000.

[6] N. Babaami, A. Zobeidi, L. Zenkheri, S. Boudjema, G. Ben Azia, and A. Benhania, "Wastewater Treatment by Improving the Local Clay Capacity with Chemical and Thermal Activation," *Asian Journal of Water, Environment and Pollution*, vol. 20, pp. 53-59, 2023.

[7] M. A. Rauf, I. Shehadeh, A. Ahmed, and A. Al-Zamly, "Removal of methylene blue from aqueous solution by using gypsum as a low cost adsorbent," *International Journal of Chemical and Molecular Engineering*, vol. 3, pp. 369-374, 2009.

[8] K. Santhy and P. Selvapathy, "Removal of reactive dyes from wastewater by adsorption on coir pith activated carbon," *Bioresource technology*, vol. 97, pp. 1329-1336, 2006.

[9] H. M. A. Shahzad, S. J. Khan, Y. Jamal, and Z. Habib, "Evaluating the performance of anaerobic moving bed bioreactor and upflow anaerobic hybrid reactor for treating textile desizing wastewater," *Biochemical Engineering Journal*, vol. 174, p. 108123, 2021.

[10] F. Qian, X. Sun, and Y. Liu, "Removal characteristics of organics in bio-treated textile wastewater reclamation by a stepwise coagulation and intermediate GAC/O3 oxidation process," *Chemical Engineering Journal*, vol. 214, pp. 112-118, 2013.

[11] S. Mabrouk, A. A. Bebba, A. Kamarchou, and A. Zobeidi, "Adsorption capacity of pollutants by using local clay mineral from urban wastewater Touggourt (South-East Algeria)," Asian Journal of Research in Chemistry, vol. 13, pp. 85-90, 2020.

[12] S. N. Malik, P. C. Ghosh, A. N. Vaidya, and S. N. Mudliar, "Hybrid ozonation process for industrial wastewater treatment: Principles and applications: A review," *Journal of Water Process Engineering*, vol. 35, p. 101193, 2020.

[13] A. Zobeidi and L. Moussaoui, "Physico-chemical quality of drinking water in the south of Algeria (Case of El-Oued region) study of excess minerals," *International Letters of Chemistry, Physics and Astronomy,* vol. 11, pp. 38--43, 2013.

[14] A. Mittal and J. Mittal, "Hen feather: A remarkable adsorbent for dye removal," *Green chemistry for dyes removal from wastewater: Research trends and applications,* pp. 409-457, 2015.

[15] A. M. Lotito, U. Fratino, G. Bergna, and C. Di Iaconi, "Integrated biological and ozone treatment of printing textile wastewater," *Chemical Engineering Journal,* vol. 195, pp. 261-269, 2012.

[16] A. Zobeidi and A. A. Bebba, "Seasonal variations of physical, chemical parameters in a wastewater treatment plant by aerated lagoons at Southern-East of Algeria," *Research Journal of Pharmaceutical, Biological and Chemical Sciences,* vol. 6, pp. 1097-1102, 2015.

[17] Z. Ammar, B. A. Abdelhafid, and D. Ali, "The effects of hydraulic retention time on organic loading rate in efficiency of aerated lagoons in treating rural domestic wastewater at el-oued (South-East Algeria)," *Orient J Chem,* vol. 33, pp. 1890-1898, 2017.

[18] G. Crini, E. Lichtfouse, L. D. Wilson, and N. Morin-Crini, "Adsorption-oriented processes using conventional and non-conventional adsorbents for wastewater treatment," *Green adsorbents for pollutant removal: fundamentals and design,* pp. 23-71, 2018.

[19] T. W. Leal, L. A. Lourenço, A. S. Scheibe, S. M. G. U. de Souza, and A. A. U. de Souza, "Textile wastewater treatment using low-cost adsorbent aiming the water reuse in dyeing process," *Journal of Environmental Chemical Engineering,* vol. 6, pp. 2705-2712, 2018.

[20] S. Biswas, J. Fatema, T. Debnath, and T. U. Rashid, "Chitosan–clay composites for wastewater treatment: a state-of-the-art review," *ACS ES&T Water,* vol. 1, pp. 1055-1085, 2021.

[21] D. Atia, A. Zobeidi, S. Neghmouche Nacer, D. Ghernaout, and N. Elboughdiri, "Biocomposite of nontronite/Enteromorpha sp. for cationic methylene blue dye removal: optimization, kinetics, and isothermal thermodynamics study," Biomass Conversion and Biorefinery, pp. 1-18, 2024.

[22] S. Mirmohamadsadeghi, T. Kaghazchi, M. Soleimani, and N. Asasian, "An efficient method for clay modification and its application for phenol removal from wastewater," *Applied Clay Science,* vol. 59, pp. 8-12, 2012.

[23] İ. Teğin and C. Saka, "Chemical and thermal activation of clay sample for improvement adsorption capacity of methylene blue," *International Journal of Environmental Analytical Chemistry,* vol. 103, pp. 4503-4514, 2023.

[24] S. Ismadji, F. E. Soetaredjo, A. Ayucitra, S. Ismadji, F. E. Soetaredjo, and A. Ayucitra, "Modification of clay minerals for adsorption purpose," *Clay Materials for Environmental Remediation,* pp. 39-56, 2015.

[25] B. Babu and S. Gupta, "Adsorption of Cr (VI) using activated neem leaves: kinetic studies," *Adsorption,* vol. 14, pp. 85-92, 2008.

[26] A. J. Baker and P. L. Walker, "Ecophysiology of metal uptake by tolerant plants," *Heavy metal tolerance in plants: evolutionary aspects,* vol. 2, pp. 155-165, 1990.

[27] C. Barranguet, B. Veuger, S. A. Van Beusekom, P. Marvan, J. J. Sinke, and W. Admiraal, "Divergent composition of algal-bacterial biofilms developing under various external factors," *European journal of phycology,* vol. 40, pp. 1-8, 2005.

[28] S. Baumont, J.-P. Camard, A. Lefranc, A. Franconi, O. r. d. s. ., and I. d. a. e. d. u. d. Î.-d.-F. . *Réutilisation des eaux usées épurées: risques sanitaires et faisabilité en Île-de-France*: ORS Ile-de-France, 2014.

[29] S. Bautista-Baños, A. N. Hernandez-Lauzardo, M. G. Velazquez-Del Valle, M. Hernández-López, E. A. Barka, E. Bosquez-Molina, *et al.*, "Chitosan as a potential natural compound to control pre and postharvest diseases of horticultural commodities," *Crop protection,* vol. 25, pp. 108-118, 2006.

[30] J.-M. Berland and C. Juery, "Les procédés membranaires pour le traitement de l'eau," *Document technique FNDAE,* vol. 14, 2002.

[31] M. Rafatullah, O. Sulaiman, R. Hashim, and A. Ahmad, "Adsorption of methylene blue on low-cost adsorbents: a review," *Journal of hazardous materials,* vol. 177, pp. 70-80, 2010.

[32] R. Mecheri, A. Zobeidi, S. Atia, S. Neghmouche Nacer, A. A. Salih, M. Benaissa*, et al.*, "Modeling and Optimizing the Crystal Violet Dye Adsorption on Kaolinite Mixed with Cellulose Waste Red Bean Peels: Insights into the Kinetic, Isothermal, Thermodynamic, and Mechanistic Study," *Materials,* vol. 16, p. 4082, 2023.

[33] A. Hamidi, D. Atia, A. Rebiai, A. Reghioua, A. Zobeidi, M. Messaoudi*, et al.*, "Investigation of adsorption kinetics and isothermal thermodynamics for optimizing methylene blue adsorption onto a modified clay with cellulose using the response surface approach," *Biomass Conversion and Biorefinery,* pp. 1-15, 2023.

[34] S. Biswas, T. U. Rashid, T. Debnath, P. Haque, and M. M. Rahman, "Application of chitosan-clay biocomposite beads for removal of heavy metal and dye from industrial effluent," *Journal of Composites Science,* vol. 4, p. 16, 2020.

[35] V. N. Tirtom, A. Dinçer, S. Becerik, T. Aydemir, and A. Çelik, "Removal of lead (II) ions from aqueous solution by using crosslinked chitosan-clay beads," *Desalination and water treatment,* vol. 39, pp. 76-82, 2012.

[36] K. T. Alben, "Books and Software: Design, analyze, and optimize with Design-Expert," ed: ACS Publications, 2002.

[37] D. Expert, "Design Expert," *Inc., Minneapolis, MN,* 2002.

[38] S. Zhu, R. Shi, J. Wang, J.-F. Wang, and X.-M. Li, "Unpredictable chronic mild stress not chronic restraint stress induces depressive behaviours in mice," *Neuroreport,* vol. 25, pp. 1151-1155, 2014.

[39] E. A. Abdelrahman, A. Alharbi, A. Subaihi, A. M. Hameed, M. A. Almutairi, F. K. Algethami*, et al.*, "Facile fabrication of novel analcime/sodium aluminum silicate hydrate and zeolite Y/faujasite mesoporous nanocomposites for efficient removal of Cu (II) and Pb (II) ions from aqueous media," *Journal of Materials Research and Technology,* vol. 9, pp. 7900-7914, 2020.

[40] M. Akbelen, "INVESTIGATION OF NATURAL ANALCIME-RICH ZEOLITE TUFF FROM TURKEY: A COMBINED XRD, XRF, FT-IR AND SEM STUDY," *Eskişehir Teknik Üniversitesi Bilim ve Teknoloji Dergisi B-Teorik Bilimler,* vol. 9, pp. 36-41, 2021.

[41] T. Chuenpratoom, K. Hemavibool, K. Rermthong, and S. Nanan, "Removal of lead by merlinoite prepared from sugarcane bagasse ash and kaolin: synthesis, isotherm, kinetic, and thermodynamic studies," *Molecules,* vol. 26, p. 7550, 2021.

[42] F. O. Omwoyo and G. Otieno, "Optimization of Methylene Blue Dye Adsorption onto Coconut Husk Cellulose Using Response Surface Methodology: Adsorption Kinetics, Isotherms and Reusability Studies," *Journal of Materials Science and Chemical Engineering,* vol. 12, pp. 1-18, 2024.

[43] S. Bahemmi, A. Zobeidi, S. Atia, S. N. Nacer, D. Ghernaout, and N. Elboughdiri, "Activating Illite kaolinite clay with CTAB for adsorbing Methylene blue: Isotherms, Kinetics, and thermodynamics studies," *Tuijin Jishu/Journal of Propulsion Technology,* vol. 44, p. 2023.

[44] I. H. Alsohaimi, M. S. Alhumaimess, A. A. Alqadami, H. M. Hassan, Q. Chen, M. S. Alamri*, et al.*, "Chitosan-carboxylic acid grafted multifunctional magnetic nanocomposite as a novel adsorbent for

effective removal of methylene blue dye from aqueous environment," *Chemical Engineering Science,* vol. 280, p. 119017, 2023.

[45] S. Bentahar, A. Dbik, M. El Khomri, N. El Messaoudi, and A. Lacherai, "Adsorption of methylene blue, crystal violet and congo red from binary and ternary systems with natural clay: Kinetic, isotherm, and thermodynamic," *Journal of environmental chemical engineering,* vol. 5, pp. 5921-5932, 2017.

[46] I. Langmuir, "The adsorption of gases on plane surfaces of glass, mica and platinum," *Journal of the American Chemical society,* vol. 40, pp. 1361-1403, 1918.

[47] J. Appel, "Freundlich's adsorption isotherm," *Surface Science,* vol. 39, pp. 237-244, 1973.

[48] R. D. Johnson and F. H. Arnold, "The Temkin isotherm describes heterogeneous protein adsorption," *Biochimica et Biophysica Acta (BBA)-Protein Structure and Molecular Enzymology,* vol. 1247, pp. 293-297, 1995.

[49] K. Foo and B. Hameed, "Coconut husk derived activated carbon via microwave induced activation: effects of activation agents, preparation parameters and adsorption performance," *Chemical Engineering Journal,* vol. 184, pp. 57-65, 2012.

[50] A. H. Jawad, A. S. Abdulhameed, N. N. Abd Malek, and Z. A. ALOthman, "Statistical optimization and modeling for color removal and COD reduction of reactive blue 19 dye by mesoporous chitosan-epichlorohydrin/kaolin clay composite," *International journal of biological macromolecules,* vol. 164, pp. 4218-4230, 2020.

[51] S. Rahmani, B. Zeynizadeh, and S. Karami, "Removal of cationic methylene blue dye using magnetic and anionic-cationic modified montmorillonite: kinetic, isotherm and thermodynamic studies," *Applied Clay Science,* vol. 184, p. 105391, 2020.

[52] N. Somsesta, V. Sricharoenchaikul, and D. Aht-Ong, "Adsorption removal of methylene blue onto activated carbon/cellulose biocomposite films: Equilibrium and kinetic studies," *Materials Chemistry and Physics,* vol. 240, p. 122221, 2020.

[53] A. H. Jawad, A. S. Abdulhameed, S. Surip, and S. Sabar, "Adsorptive performance of carbon modified chitosan biopolymer for cationic dye removal: kinetic, isotherm, thermodynamic, and mechanism study," *International Journal of Environmental Analytical Chemistry,* vol. 102, pp. 6189-6203, 2022.

[54] M. I. Khan, "Adsorption of methylene blue onto natural Saudi Red Clay: isotherms, kinetics and thermodynamic studies," *Materials Research Express,* vol. 7, p. 055507, 2020.

[55] P. W. Atkins and M. J. De Paula, *Chimie physique*: De Boeck Supérieur, 2013.

[56] S.-K. Zhou, Y.-J. Liu, H.-Y. Jiang, W.-J. Deng, and G.-M. Zeng, "Adsorption of U (VI) from aqueous solution by a novel chelating adsorbent functionalized with amine groups: equilibrium, kinetic, and thermodynamic studies," *Environmental Engineering Science,* vol. 35, pp. 53-61, 2018.

[57] S. K. Singh and A. Das, "The n→ π* interaction: a rapidly emerging non-covalent interaction," *Physical Chemistry Chemical Physics,* vol. 17, pp. 9596-9612, 2015.

[58] H. L. Parker, A. J. Hunt, V. L. Budarin, P. S. Shuttleworth, K. L. Miller, and J. H. Clark, "The importance of being porous: polysaccharide-derived mesoporous materials for use in dye adsorption," *RSC advances,* vol. 2, pp. 8992-8997, 2012.